New Phytologist

Research

Starch and lipid storage strategies in tropical trees relate to growth and mortality

David Herrera-Ramírez[1], Carlos A. Sierra[1], Christine Römermann[2,3], Jan Muhr[1,4], Susan Trumbore[1], Divino Silvério[5], Paulo M. Brando[6,7,8] and Henrik Hartmann[1]

[1]Max Planck Institute for Biogeochemistry, Hans-Knöll-Str 10, Jena 07745, Germany; [2]German Centre for Integrative Biodiversity Research (iDiv) Halle-Jena-Leipzig, Leipzig D-04103, Germany; [3]Department of Bioclimatology, Georg August University Göttingen, Büsgenweg 2, Göttingen 37077, Germany; [4]Institute of Ecology and Evolution, Friedrich Schiller University Jena, Philosophenweg 16, Jena 07743, Germany; [5]Department of Biology, Universidade Federal Rural da Amazônia – UFRA, Capitão Poço, Pará 68650-000, Brazil; [6]Department of Earth System Science, University of California, Irvine, CA 92697, USA; [7]Instituto de Pesquisa Ambiental da Amazônia, Brasília, DF 70863-520, Brazil; [8]Woodwell Climate Research Center, Falmouth, MA 02540, USA

Author for correspondence:
David Herrera-Ramírez

Received: *26 July 2020*
Accepted: *11 December 2020*

New Phytologist (2021) **230:** 139–154
doi: 10.1111/nph.17239

Key words: neutral lipids, non-structural carbohydrates (NSC), starch, wood anatomy, wood carbon storage, wood traits.

Summary

- Non-structural carbon (NSC) storage (i.e. starch, soluble sugras and lipids) in tree stems play important roles in metabolism and growth. Their spatial distribution in wood may explain species-specific differences in carbon storage dynamics, growth and survival. However, quantitative information on the spatial distribution of starch and lipids in wood is sparse due to methodological limitations.
- Here we assessed differences in wood NSC and lipid storage between tropical tree species with different growth and mortality rates and contrasting functional types. We measured starch and soluble sugars in wood cores up to 4 cm deep into the stem using standard chemical quantification methods and histological slices stained with Lugol's iodine. We also detected neutral lipids using histological slices stained with Oil-Red-O.
- The histological method allowed us to group individuals into two categories according to their starch storage strategy: fiber-storing trees and parenchyma-storing trees. The first group had a bigger starch pool, slower growth and lower mortality rates than the second group. Lipid storage was found in wood parenchyma in five species and was related to low mortality rates.
- The quantification of the spatial distribution of starch and lipids in wood improves our understanding of NSC dynamics in trees and reveals additional dimensions of tree growth and survival strategies.

Introduction

In trees, non-structural carbon (NSC) stored mainly in the form of starch, soluble sugars and lipids can be remobilized during periods of carbon limitation to support tree metabolism (Chapin *et al.*, 1990; Hoch *et al.*, 2003; Begum *et al.*, 2010). Storage remobilization can occur on different timescales and may allow trees to grow, respire and build defence compounds during the night (Sulpice *et al.*, 2009; Tixier *et al.*, 2018). It can also support metabolism during seasonal or occasional stressful conditions that limit carbon assimilation, such as drought, floods or physical damage (McDowell *et al.*, 2008; Hartmann & Trumbore, 2016). Thus, tree growth and survival under these limiting conditions may be linked to the amount of stored reserves and the capacity to remobilize storage (Sala *et al.*, 2012). Tree survival during drought has already been linked to storage content in seedlings of tropical trees (O'Brien *et al.*, 2014, 2020). Nevertheless, these links are not well understood in adult tropical trees, principally due to the following factors: first, the influence of other tree traits such as xylem vulnerability to embolism, rooting depth or wood density on plant survival (McDowell *et al.*, 2008; Johnson *et al.*, 2012; Rowland *et al.*, 2015; Boonman *et al.*, 2020; Borghetti *et al.*, 2020); and, second, lack of understanding of NSC storage regulation (Dickman *et al.*, 2019).

In addition to providing carbon reserves during periods of low carbon supply from photosynthesis, NSC also plays other important roles in trees. For instance, starch synthesis and degradation are key factors in the regulation of water potential in plant tissues to avoid cell desiccation and cavitation in the xylem, and to remove embolisms following cavitation (Salleo *et al.*, 2009; Lintunen *et al.*, 2016; Savi *et al.*, 2016). Starch metabolism also serves as a regulator of processes that control plant growth, defense and development (Sulpice *et al.*, 2009;

Dedication: This article is dedicated to Professor Fritz Hans Schweingruber 1936–2020: his wise guidance, curiosity and deep love for wood remain a source of inspiration.

Smirnova *et al.*, 2015). Non-structural carbon content in plant tissues represents both an indicator of the status of a tree's carbon balance and a predictor of biomass growth and other metabolic traits (Sulpice *et al.*, 2009; Gérard & Bréda, 2014). Thus, its precise localization and quantification may mirror a tree's overall metabolic strategy.

Starch is stored in semi-crystalline grains in the plastid stroma of living cells in all tree organs (e.g. leaves, stems and roots). In wood, starch is generally synthesized and stored in the plastids of living parenchyma cells (Spicer, 2014; Plavcová & Jansen, 2015; von Arx *et al.*, 2017; Tixier *et al.*, 2018), but living fibers may also store important amounts of starch (Carlquist, 2013, 2015; Plavcová *et al.*, 2016). However, the role of living fibers in tree storage dynamics remains unexplored. Living fiber cells originate from the fusiform cambial initials and keep their protoplasts alive from one to several years after maturation (Fahn & Arnon, 1963; Yamada *et al.*, 2011; Carlquist, 2013, 2015). In comparison with axial parenchyma, these fibers are not subdivided into strands, are usually septated, have thicker cell walls, and have fewer and smaller pits that reduce their intercellular communication and may slow down the remobilization of hydrolyzed starch (Carlquist, 2013, 2015). If present, living fibers may play an important role in carbon storage dynamics of trees. For instance, higher allocation of starch to living fibers may increase storage capacity due to the high volume of fibers in wood, but it may slow down its remobilization due to their reduced intercellular communication. Exclusive storage in parenchyma cells may limit total storage capacity, but starch hydrolysis and remobilization may be easier and faster to export to neighboring cells, probably due to the high number of large pits of parenchyma cells. Consequently, these anatomical constraints on NSC storage and remobilization may also affect the growth and survival of plants. Despite the fact that the occurrence of living fibers has been reported for several tree species (Carlquist, 2013, 2015; Plavcová *et al.*, 2016), their presence in tropical trees and their role in NSC storage and remobilization dynamics remain to be investigated.

Woody organs constitute potentially the largest long-term reservoir of starch in trees (Würth *et al.*, 2005; Chesney & Vasquez, 2007; Furze *et al.*, 2018, 2019; O'Brien *et al.*, 2020). In general, starch concentration is highest in the youngest wood, close to the phloem, and decreases radially towards the pith (Saranpää & Höll, 1989; Hoch *et al.*, 2003; Gérard & Bréda, 2014). However, this pattern is highly variable among species – some may store starch in deeper wood layers or in higher concentrations than other species (Würth *et al.*, 2005; Furze *et al.*, 2020). In coarse roots, which are woody organs, the storage size seems to be a better predictor of tree survival than the NSC concentrations alone (Wiley *et al.*, 2019). This may be also the case for other woody organs such as stems and branches. Therefore, accounting for the spatial distribution of storage compounds in the stem wood would improve the estimation of NSC-pool size, our understanding of storage dynamics in adult trees, and our understanding of tree growth and survival.

In addition to starch, neutral lipids also play a major role as storage compounds in some tree species and can thus be important for maintaining the carbon balance and important metabolic functions (Schneider *et al.*, 2003; Begum *et al.*, 2010; Fischer *et al.*, 2015; Welte & Gould, 2017). Based on the abundance of lipids in wood, trees have been classified into two groups of storage strategy: fat storing trees (abundant lipid storage) and starch storing trees (scarce lipid storage) (Hillinger *et al.*, 1996; Hoch *et al.*, 2003; Hartmann & Trumbore, 2016). However, lipid content has been studied in only a few temperate species because of difficulties related to its quantification and detection (Höll & Poschenrieder, 1975; Fischer & Höll, 1991; Hoch *et al.*, 2003). Considering the high abundance of parenchyma tissue and low concentrations of starch in tropical trees (Plavcová *et al.*, 2016), one would expect that lipids may play an important role in the long-term carbon storage for these tree species; however, the spatial distribution of lipid pools has been described for only a few species (Datta & Kumar, 1987; Nobuchi *et al.*, 1996). This greatly limits our understanding of storage strategies in trees, and can also lead to underestimations of the carbon storage pool size in trees and forests.

Quantification of the spatial distribution of storage compounds using the available analytical methods is challenging. Recently, standard methods have been proposed to reduce analytical errors and produce consistent NSC measurements across laboratories (Landhäusser *et al.*, 2018). However, these wet chemistry approaches quantify NSC in the bulk wood mass, irrespective of the spatial distribution or wood cell types in which NSC are actually stored. By contrast, approaches such as micro computerized tomography (Earles *et al.*, 2018) and histological techniques on wood anatomy in combination with image analysis (Begum *et al.*, 2010; Czemmel *et al.*, 2015) offer a great opportunity to quantify the spatial distribution of storage compounds and concentration gradients across different wood cell types.

In this paper we address the following question: what are the differences in wood storage traits between tropical trees with contrasting life history traits? To do this, we compared a selected group of evergreen and semi-deciduous trees with different growth and mortality rates. In particular, we hypothesize the following: first, trees from fast-growing, short-lived species store starch mainly in parenchyma cells and have lower NSC concentrations, serving as a short-term buffer against diel and intraseasonal carbon shortages; second, by contrast, trees from slow-growing, long-lived species store a high proportion of starch in living fibers in the wood, as they store more NSC for supporting metabolism and growth during extreme carbon shortages. To test these hypotheses, we used histological and chemical methods to quantify the starch content and spatial distribution in the wood of mature trees, and to assess both presence and localization of starch and lipids in different wood cell types.

Materials and Methods

Study site and plant material

This study was conducted at a seasonally dry forest in the transition zone between Amazon rainforests and Cerrado in central

Table 1 Descriptions of the samples.

Species name	Family	Order	Clades	Storage strategy	Growth rate (cm yr^{-1})	Mort. rate (% yr^{-1})	Functional type	No. ind. (HPAE)	No. ind. (Hist)	No. samp. (HPAE)	No. samp (Hist)
Ocotea leucoxylon (Sw.) Laness	Lauraceae	Laurales	Magnoliids	Parenchyma	0.17	5.7	Evergreen	5	4	10	7
Ocotea guianensis Aubl.	Lauraceae	Laurales	Magnoliids	Parenchyma	0.22	4.1	Evergreen	5	3	10	6
Sacoglottis guianensis Benth.	Humiriaceae	Malpighiales	Eudicots(core eudicots(rosids (fabids)))	Parenchyma	0.29	5	Semi-deciduous	5	3	10	5
Schefflera morototoni (Aubl.) Maguire, Steyerm & Frodin	Araliaceae	Apiales	Eudicots(core eudicots (asterids (campanulids)))	Parenchyma	0.60	1.9	Semi-deciduous	5	0	10	0
Vochysia vismiifolia Spr. Ex Warm.	Vochysiaceae	Myrtales	Eudicots(core eudicots(rosids (malvids)))	Parenchyma	0.81	3.1	Semi-deciduous	5	3	10	5
Dacryodes microcarpa Cuart.	Burseraceae	Sapindales	Eudicots(core eudicots(rosids (malvids)))	Fibers	0.10	1.6	Semi-deciduous	5	2	10	2
Tapirira guianenesis Aubl.	Anacardiaceae	Sapindales	Eudicots(core eudicots(rosids (malvids)))	Fibers	0.25	2.5	Semi-deciduous	5	3	10	5
Trattinnickia burserifolia Mart.	Burseraceae	Sapindales	Eudicots(core eudicots(rosids (malvids)))	Fibers	0.21	1.0	Evergreen	5	1	10	2
Trattinnickia glaziovii Swart.	Burseraceae	Sapindales	Eudicots(core eudicots(rosids (malvids)))	Fibers	0.06	1.7	Evergreen	5	2	10	4

The number of samples per species considers the two wood depths analyzed, from 0 to 2 cm and from 2 to 4 cm deep, in the wood. The number of samples differs between the two quantification methods because of the loss of samples due to processing problems or fungus infection. Hist., histological quantification method; HPAE, high-performance anion exchange chromatography with pulsed amperometric detection quantification method; Mort. rate, mortality rate; No. ind., number of individuals per species used for quantification; No. samp., number of samples per species used for quantification.

Brazil (Table 1), at the Tanguro Ranch in the state of Mato Grosso (lat 13°4′ 35.39″S, long 52°23′ 8.85″W). We sampled individuals from nine dominant tree species within a 50 ha plot that served as a control in the fire frequency experiment described in Balch *et al.,* (2008), and where species-specific growth and mortality rates were measured. The region has mean annual temperature and precipitation values of 25°C and 1770 mm, respectively (Rocha *et al.*, 2014). A marked dry season occurs between the months of May and August with rainfall of < 10 mm $month^{-1}$ (Rocha *et al.*, 2014).

We collected samples during the rainy season (in January 2018). From each tree species, we chose mature, dominant, and healthy trees with a diameter at breast height (1.3 m, dbh) larger than 20 cm (Table 1). Within this group of individuals we chose five random trees per species. We selected species of two contrasting functional types (evergreen and semi-deciduous) and with different growth and mortality rates for comparison of starch and lipid concentrations in stem wood (Table 1). Additionally, we resampled the same trees in July 2018, during the dry season, to identify the starch location in the wood, although no quantification of NSC was done on these samples.

Growth and mortality rates

Annual growth and mortality rates for each species were calculated based on forest inventories conducted between 2004 and 2018 (Balch *et al.*, 2011; Brando *et al.*, 2019; Table 1). All trees with dbh ≥ 40 cm were measured. Nested sub-samplings over transects of 500 × 20 m were done to sample smaller trees and lianas with dbh ≥ 1cm (see Balch *et al*, 2011 for details). To estimate mortality and growth rates, dbh and mortality data were recorded annually between 2004 and 2010 and every 2 yr from 2012 to 2018 (Balch *et al.*, 2011; Brando *et al.*, 2019). Mortality was estimated by applying a 0–5 categorical scale for assessing aboveground tissue: 0 corresponded to no visible aboveground live tissue, and 5 corresponded to 100% of all visible above ground tissue alive. Most of the species selected had > 100 individuals when the inventories started in 2004, with only three exceptions: *Schefflera morototoni* (Aubl.), *Dacryodes microcarpa* Cuart. and *Vochysia vismiifolia* Spr. Ex Warm. had 18, 62, and 45 individuals, respectively (Balch *et al.*, 2011). Annual growth rates were estimated for each species from changes in dbh for all individuals with dbh ≥ 20 cm (Brando *et al.*, 2019). We used

the median of the growth rates as an estimate of the annual growth rate for each species.

Sampling procedure

From each individual tree, we extracted two wood cores (5 mm diameter and 6 cm long) from bark to pith using an increment borer (Supporting Information Methods S1). The increment cores were taken at the same height (1.3 m), 5 cm apart from each other (horizontally). The cores were placed in ice immediately after collection and frozen at −18°C within 2 h. They were kept frozen until it was possible to dry them in an oven at 60°C for 2 d. Before placing them in the oven, the cores were microwaved for 3 min at 500 W (Landhäusser *et al.*, 2018). We used one of the two cores for quantifying starch and soluble sugars with chemical extraction and ion chromatography (IC), employing high-performance anion exchange chromatography with pulsed amperometric detection (HPAE-PAD, Dionex ICS-3000 with CarboPac columns, Dionex, CA, USA). We followed the specifications outlined in an earlier article (see Protocol S3 in Landhäusser *et al.*, 2018). We used the second core to visualize and quantify starch and lipids in histological slides of the cross-sectional area of the wood. Each increment core was divided into two sections to account for the concentration of starch in increments of 2 cm starting at the cambium (two depth ranges: 0–2 and 2–4 cm).

Extraction and quantification of soluble sugars and starch

The 2-cm long core sections were ground to a fine powder using a ball mill (MM 400, Retsch, Haan, Germany) at 25 Hz for 30 s. We extracted the soluble sugars from each sample following a previously described method (Protocol S1 in Landhäusser *et al.*, 2018). We dried 50 mg of wood powder at 60°C overnight. Dry samples were boiled in 1.5 ml of 80% ethanol for 10 min at 90°C. After cooling to room temperature, the samples were centrifuged at 13 000 ***g*** for 2 min. The supernatant was recovered in a new vial and stored frozen for posterior quantification of soluble sugars. Before measurement, the supernatant was diluted, filtered, and then used for measuring three specific sugars (sucrose, fructose and glucose) by HPAE-PAD. For quality control we used blanks and standard solutions with known concentrations of glucose, fructose and sucrose, as described previously (see Protocol S3 in Landhäusser *et al.*, 2018). The measurement of each sugar was reported in units of mg l^{-1}, and then transformed to percentage (w/w) of soluble sugars as:

$$\%\text{sugar} = \frac{([\text{glucose}] + [\text{fructose}] + [\text{sucrose}]) \cdot 1.05 \cdot V_{\text{extract}} \cdot df}{W \cdot 10^3} \cdot 100\%$$

where [glucose], [fructose] and [sucrose] are the concentration of each soluble sugar in mg l^{-1}, respectively, and obtained from the HPAE-PAD; V_{extract} is the volume of ethanol–water in ml used for the extraction, df is the dilution factor used for each particular sample, W is the dry weight of the sample in mg, and 1.05 is a correction factor (Landhäusser *et al.*, 2018).

For starch quantification, in the remaining pellet, two additional soluble sugar extractions were performed as described here, each time discarding the supernatant to remove any remaining soluble compounds that may interfere with the quantification. The pellet then was dried overnight at 60°C to remove residual ethanol. We used the enzymatic digestion method described in an earlier study (see Protocol S2 in Landhäusser *et al.*, 2018) to extract the starch. We converted starch into soluble oligosaccharides by adding 1 ml of α-amylase (600 units ml^{-1}) from *Bacillus licheniformis* (cat. no. A4551; Sigma) to the dry pellet. Samples were incubated in an orbital shaker for 1 h at 85°C. Then the samples were left to cool down to room temperature and centrifuged at 13 000 ***g*** for 3 min. The supernatant was transferred to a new 2 ml screw-cap microcentrifuge tube. The oligosaccharides in the supernatant were hydrolysed into glucose by adding 0.5 ml of amyloglucosidase solution (12 units ml^{-1}) followed by incubation at 55°C for 30 min. Afterwards, enzymes were precipitated from the solution with chloroform. The remaining solution was diluted by a factor of 10 (i.e. 1 : 10 dilution) with distilled water and filtered to further clean it. The glucose in the solution was then measured by HPAE-PAD and recorded in units of mg l^{-1}. Here we used the glucose standard solutions for quality control. These values were transformed to percentage of starch (i.e. grams of starch per 100 g of dry wood (gdw) as follows:

$$\%\text{starch} = \frac{[\text{glucose}] \cdot V_{\text{starch}}}{W \cdot 10^3} \cdot 0.9 \cdot 100\%$$

where V_{starch} is the volume of the solution used for the extraction and 0.9 is a correction factor for mass gain during hydrolysis (Landhäusser *et al.*, 2018).

Histological visualization and quantification of starch

Each 2-cm long section from the second increment core was sliced perpendicularly to the axial oriented fibers using an electronic rotatory microtome (HM 340E; Thermo Fisher Scientific, Waltham, MA, USA). We took 30 μm thick histological slices, following the guidelines given by von Arx *et al.* (2016), aiming to obtain a slice of even thickness (Methods S1). The slices were mounted on a glass slide with glycerol, covered with Lugol's iodine solution for 3 min to stain starch grains, and finally covered with a glass plate. The stained samples were photographed using an optical digital microscope with a large depth-of-field (VHX-6000; Keyence, Itasca, IL, USA) within 3 h. Despite the fact that the sample handling and storage processes were treated with the utmost care, fungus contamination prevented us from using the histological method to quantify starch in all individuals of *S. morototoni* and in some individuals of other species (Table 1).

Panoramic images of the sample were taken at ×300 magnification, with both stereo and background illumination at high light intensity to maximize the contrast between the stained starch granules and the surrounding tissue. We used a large depth of field to focus on all objects at different depths in the sample. These images allowed us to identify and distinguish among wood

tissues (parenchyma, fibers and vessels), determine the area of each tissue type, and locate and determine the area covered by starch grains (starch coverage) within each tissue type (Fig. 1 left panel). This analysis also allowed us to identify the starch storage location in wood, and to characterize species by the cell types they used for starch storage in wood.

We quantified the percentage of starch in the samples by measuring repeatedly the areal percentage of starch coverage in 1 mm^2 squares across the surface of the wood sections using ImageJ (Schneider *et al.*, 2012). We divided the images into radial increments of 5 mm from bark to pith to achieve better precision in quantifying the radial distribution of starch in the stem-wood. While doing so, we also eliminated artifacts from the images that may have interfered with the quantification (Fig. 1, left panel). After having prepared the images, we ran an automatic script for identifying and quantifying starch grains in multiple 1-mm^2 regions of interest (ROI), randomly selected from across the images (Methods S2). After identifying all the starch grains in an ROI, the script measures the percentage of the surface covered by starch (Fig. 1, right panel). We measured 50 ROIs in each image of 5 mm of the stem increment core. We used the average of these 50 ROI measurements as an estimate of the starch percentage for each of the 5 mm sections of the increment core. We estimated the starch percentage in each 2-cm long section by taking the average of the percentage of the surface covered by starch in all the ROIs from the corresponding images. These measurements were our sample replicates for the validation of this quantification method with the HPAE-PAD.

Furthermore, we made manual measurements of the starch percentage in the fractional area of each wood tissue (fibers and parenchyma). For this, we outlined manually the cell type areas in the images of wood samples and generated new images corresponding to each wood-cell type: fibers, parenchyma and vessels. We then measured the amount of starch in each wood-cell type applying the same algorithm described in the previous section to each of the newly generated images. We did this only in one individual per species and only in the first 2 cm of the wood core. These measurements were used as reference values for the relative amount of starch stored per tissue type in each species.

Staining of neutral lipids

We used Oil Red O (ORO) staining on wood histological slices to detect neutral lipid droplets in wood following the protocol described in Mehlem *et al.* (2013). We prepared the ORO stock solution, adding 2.5 g of ORO to 400 ml of 99% (v/v) isopropyl alcohol and mixing the solution for 2 h at room temperature. From the stock solution, we prepared an ORO working solution, adding 1.5 parts ORO stock solution to 1 part distilled water, shaking it for 5 min, letting it stand for 10 min at room temperature, and filtering it through a 45 μm filter to remove the precipitates.

From each 2-cm long section of the second core, we cut a new histological slice subsequent to the one taken for starch measurements, following the same guidelines described in the previous section. The histological slices were washed with distilled water and then placed in a Petri dish. Next, 1 or 2 ml of ORO working solution was added to completely cover the samples. We fixed a lid onto the Petri dish to avoid drying of the ORO solution, and let the sample incubate for 30 min at room temperature. Samples were then rinsed with distilled water for *c.* 30 min, mounted on the slides using water as a mounting medium, and placed under a coverslip. Pictures were taken within 1 h, before the water dried out and the ORO started to precipitate. The samples were photographed using the optical digital microscope at ×500 magnification. We did not quantify the neutral lipid content based on these images due to its lack of comparability with the starch quantification and the lack of a calibration method. However, these images allowed us to demonstrate whether or not the species contained lipids, to detect where the lipids were stored in the xylem, and to investigate whether lipids contribute to the storage pool in our trees.

Statistical analysis

To validate the histological method with HPAE-PAD we ran a simple linear model between the two measurements of starch concentration, the percentage of starch per unit mass (from the HPAE-PAD quantification) as the independent variable, and the percentage of starch per unit area (obtained from the histological samples) as the dependent variable. The data met all the statistical requirements, such as normal distribution of the residuals and homoscedasticity. We also tested the effect of the species and depth range on the slope and the intercept of the linear model using ANCOVA. This model allowed us to scale the measurements from the histological method to the units that the HPAE-PAD quantification reports. In addition, we ran permutation tests to evaluate with 95% confidence whether the slope of the linear model was different from zero, and if the means of the two quantification methods differed from each other.

To evaluate the relationship between the starch storage location observed in the histological images and the functional types of our tree species, we used a Fisher's exact test. For comparing the growth and mortality rates between the starch storage location we used a Mann–Whitney *U*-test. We used this test because the data was not normally distributed. For the comparison, trees were classified as either trees that use living fiber for storing starch or trees that use only parenchyma.

To investigate differences in storage location and distribution of starch between individuals from different species, we estimated the probability density distribution of the percentage of starch of the wood area as a measure of the spatial distribution of the starch for the first 2 cm of wood in each species. For this, we used the starch measurements from ROIs in all individuals per species and estimated the density distribution per species using the R function *density*, which computes a kernel density estimate. These distributions gave us the relative probability of a specific starch percentage occurring along the radial profile of the wood sample. These starch distributions were compared by estimating the percentage overlap of the common area between two starch density distributions. We tested the relationship of these distributions with growth and mortality rates using linear regressions and permutation tests over the regression slope.

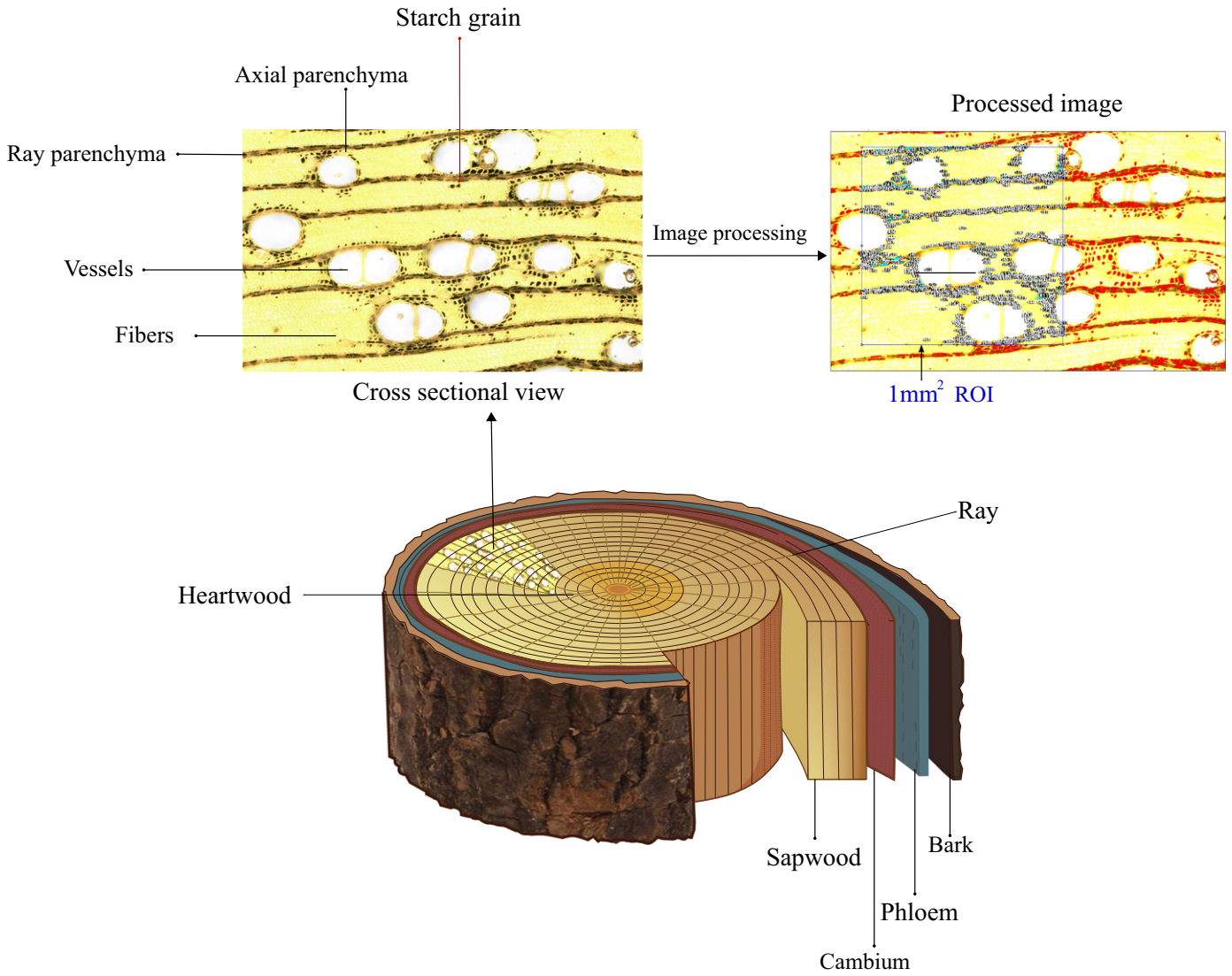

Fig. 1 Representation of the cutting plane of the samples and examples of the images of the histological slide from *Ocotea leucoxylon*, where the rays are stained brown and the starch black (left panel), and the result from the image processing, where the stained starch was recolored in red (right panel). Within a randomly chosen 1 mm^2 area (blue square) all pixels stained red were then automatically identified for measurement (selected pixels here are highlighted in black and white) using our ImageJ macros (see Supporting Information Methods S2). ROI, region of interest.

We tested the influence of the lipid storage on growth and mortality rates using the Mann–Whitney *U*-test. For this, the species were classified as species with lipid storage (species that showed consistent lipid droplets in the parenchyma cells) and species with no lipid storage (species that showed no lipid droplets in the parenchyma cells, or showed them in some sparse specific locations).

All the statistical analyses were conducted in R v.3.6.1 (R Core Team, 2017).

Results

Starch and soluble sugar partitioning

The starch content in our trees ranged from 0.1% to 15% of the dry mass (Fig. 2). Starch was the most abundant storage compound for most of the sampled trees, representing at least 70% of the total NSC, but was practically absent in individuals of *S. morototoni* and *V. vismiifolia*.

The soluble sugar content of the outermost 4 cm of stem wood ranged between 0 and 3% of the dry mass without a clear relationship with stem depth for any of the trees (Fig. 2). For most trees, soluble sugars represented < 30% of the total NSC in their wood, with the exception of individuals of *S. morototoni* and *V. vismiifolia*, whose soluble sugars were the main storage compound, representing 54% and 99.9% of the total NSC, respectively. Nevertheless, trees from these two species also had the lowest concentrations of total NSC (soluble sugars and starch), 3% and 2% respectively.

Validation of the histological method

Starch quantities determined using the histological method and the HPAE-PAD were highly correlated, and the model's slope

was very close to one ($y = 0.47 + 0.89x$, $r^2 = 0.80$, $P < 0.005$, $R = 0.89$, RMSE = 0.55, Fig. 3). No effect of tree species or the depth range on the model's slope and intercept was found ($P = 0.27$). Permutation tests confirmed these results. We found that the slope of the linear model was significantly different from zero ($P < 0.01$) and the difference in the means of the two quantification methods (0.09) was not different from zero with 95% confidence. The histological method can therefore be used not only to estimate starch concentrations but also starch spatial distribution in the wood and concentration gradients among different wood cell types.

Starch storage strategies and life history traits

Based on the location of starch in the wood, which was visible in the histological stained samples, we were able to differentiate two distinct storage strategies among individuals of the nine species evaluated. All individual trees belonging to a particular species shared the same storage strategy. One group of trees used exclusively the ray and axial parenchyma to store starch (Fig. 4 left-hand side). This group generally had low starch contents, and high annual growth and mortality rates (Fig. 5). The second group mostly used living fibers for starch storage (Fig. 4 right-hand side). In this group, we found trees that generally had a high concentration of starch, and low annual growth and mortality rates (Fig. 5). Starch concentration per wood-cell type manually measured in some histological samples showed us that for this group, between 50 and 80% of the starch was stored in the living fibers; the rest was stored in ray and axial parenchyma. These storage strategies were consistent between seasons, with all trees from a particular species showing the same storage strategy in both rainy and dry seasons (Fig. S1).

These storage strategy groups showed a weak relationship with annual growth rates ($P = 011$, Fig. S2) and a significant relationship with mortality rates ($P = 0.03$, Fig. S2). Fiber-storing trees tended to grow slower (< 0.25 cm yr^{-1}) and have lower mortality (< 3% yr^{-1}) than parenchyma storing trees (Fig. S2). Curiously, the starch storage strategies or the amount of starch stored in the wood were not related to the functional type (evergreen or semi-deciduous) of the species ($P = 0.75$, Fig. 4).

Distribution of starch in the wood

Starch content decreased radially, from the youngest wood to 4 cm depth, for many trees (Fig. 6). However, there was large variation among individuals of different species: for individuals of *Ocotea leucoxylon*, *Trattinnickia glaziovii* and *Tapirira guianensis*, starch concentrations declined gradually within the first radial 4 cm of stem-wood; for individuals of *Sacoglottis guianensis* there was a sudden decrease in starch concentration in wood beyond 3 cm; and for individuals of *Ocotea guianensis, Trattinnickia burserifolia* and *V. vismiifolia* there was no decline to 4 cm depth. For most individuals of these species, we found that deeper wood layers were completely void of starch.

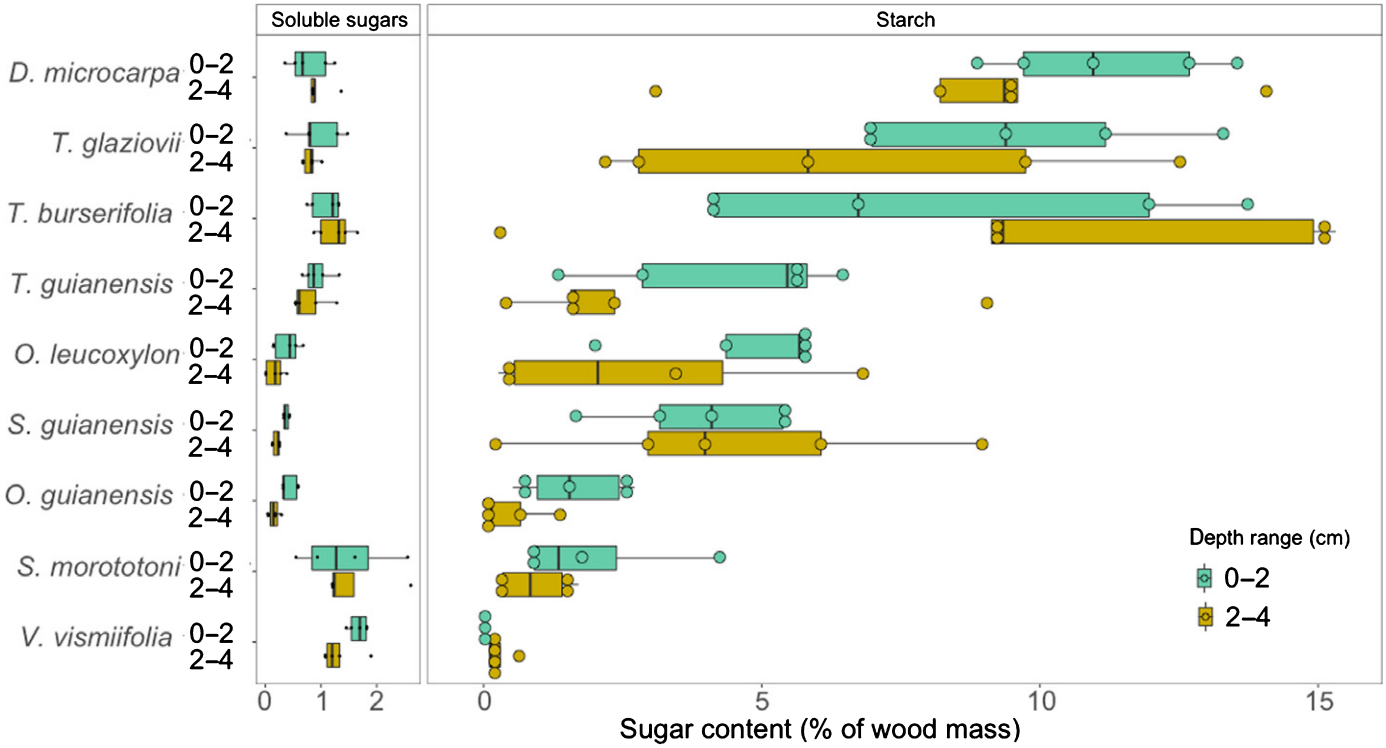

Fig. 2 Sugar and starch content (%) measured by the HPAE-PAD method for each species in the two wood depth ranges evaluated (0–2 cm and 2–4 cm deep in the wood). The boxes of the boxplots represent the 25th, 50th and 75th percentiles from left to right. The boxplot whiskers represent 1.5 × the interquartile range below the 25th percentile (left whisker), and 1.5 × the interquartile range above the 75th percentile (right whisker). The measured values are represented by the filled circles.

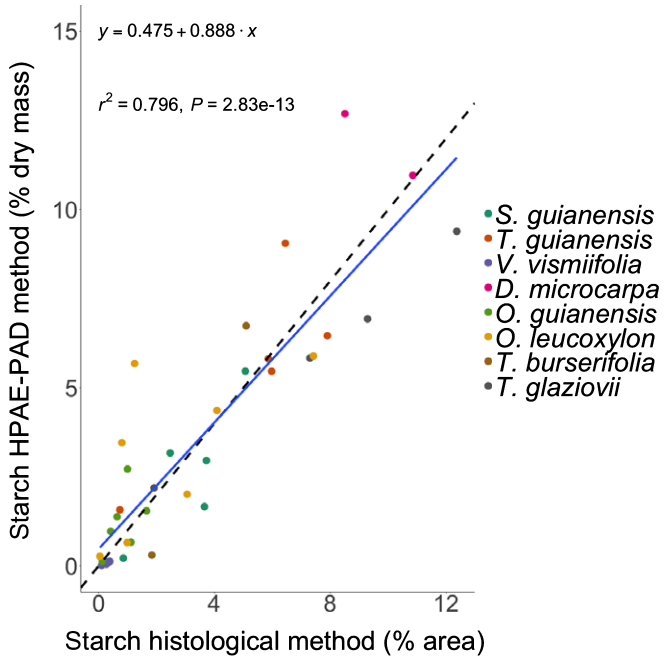

Fig. 3 Linear model fitted between the two starch quantification methods (solid blue line): the chemical extraction and high-performance anion exchange chromatography with pulsed amperometric detection (HPAE-PAD) method (*y*-axis), and the histological method (*x*-axis). Dots represent every sample from each individual of each species from the depth range analyzed. The dashed line corresponds to the 1 : 1 linear relationship that would be expected if there were complete equivalence between the methods. Different colors represent different species.

The density distributions of the percentage of starch in the first 2 cm of the stem wood in the radial direction showed two general shape types (Fig. 7). Individuals from the species that store starch only in the parenchyma had narrow distributions skewed to low values of starch content, reflecting the grouped pattern of starch in the stem parenchyma cells. By contrast, individuals from species that store starch mostly in the fibers had a more spread unimodal distribution with long tails towards high concentration values, reflecting a more dispersed pattern of starch in the wood (Fig. 7). The overlapping index between the starch distributions of the parenchyma-storing trees and the fiber-storing trees showed that both distributions share *c.* 39% of common area with an absolute error smaller than 2.9×10^{-5} (Fig. S3).

Descriptive variables from these distributions were also related to growth and mortality rates (Figs S4 and S5). The median of the percentage of starch in the wood was nonlinearly associated with growth (Fig. S4), but it was not related to mortality. Nevertheless, the cumulative mean percentage of starch from each 5 mm segment along the radial profile, up to 4 cm of the wood core, was significantly related to mortality rates ($r = 0.76$, $P = 0.036$, Fig. S5a).

Presence and localization of neutral lipids in the wood

Lipid droplets were exclusively present in parenchyma cells of individuals from five species (Fig. 8, left-hand side). The wood in individuals of the other four species was mostly void of neutral lipid droplets. In these species, lipid droplets were detected sporadically and localized only in the cell walls of vessels and in the parenchyma cells next to vessels in individuals of *T. guianensis* and *S. guianensis*; and also in secretory cells in individuals of *O. guianensis* and *O. leucoxylon*.

Lipid storage was not related to functional type or growth rates ($P > 0.1$), but it was related to mortality rates ($P = 0.031$, Fig. S2): individuals with lipid storage belong to species that had lower mortality rates (< 3% yr^{-1}) than individuals with no lipid storage.

Discussion

Using the histological method, we identified the location of starch storage and quantified its spatial distribution. This allowed us to quantify differences in wood storage traits (e.g. starch distribution) and to relate these traits to two life history traits – tree growth and mortality of nine tropical species. Our results point to two contrasting patterns. Fast-growing, short-lived species stored starch mainly in the parenchyma, while slow-growing, long-lived species stored a large proportion of starch dispersed in living wood fibers. We also found a positive relationship between lipid content and mortality rates. These results may be indicative of more general patterns of carbohydrate and lipid storage associated with life history traits such as growth, carbon allocation, and mortality. However, future studies, including species from different forest sites, are needed for broader extrapolation of our findings.

Storage strategies and life history traits

Trees that belonged to slow growing, long-lived and high-survival species stored a large proportion of their starch reserves in the living fibers in the wood and had the biggest NSC pool. Trade-offs between survival and growth have been reported for several tree species, where species that allocate more resources to high survival traits such as defense compounds and high wood density tend to grow slower than species with less allocation to survival traits (Gilbert *et al.*, 2006; Poorter *et al.*, 2008; Wright *et al.*, 2010; Adler *et al.*, 2014; Philipson *et al.*, 2014; Osazuwa-Peters *et al.*, 2017; Borghetti *et al.*, 2020). Our results showed that storage of starch in living fibers in stem wood may also be an important trait of species that prioritize allocation of resources to increase survival rather than growth. It is likely that a large number of living fibers allows high amounts of starch to be stored in the wood, which provides an efficient means by which to optimize storage capacity without sacrificing structural resistance. This may allow trees to have bigger reserve pools for the following purposes: to invest more carbon in survival traits such as the possession of an abundance of defence compounds and high wood density; to sustain metabolism during carbon shortages; and to reduce stem water potential and avoid cavitation by hydrolyzing starch. These results agree with previous findings, where concentrations of NSC correlated positively with survival rates and negatively with growth in seedlings of some tropical tree species (Poorter & Kitajima, 2007; O'Brien *et al.*, 2014, 2020). Storage allocation to living fibers has been reported before for few species (Fahn &

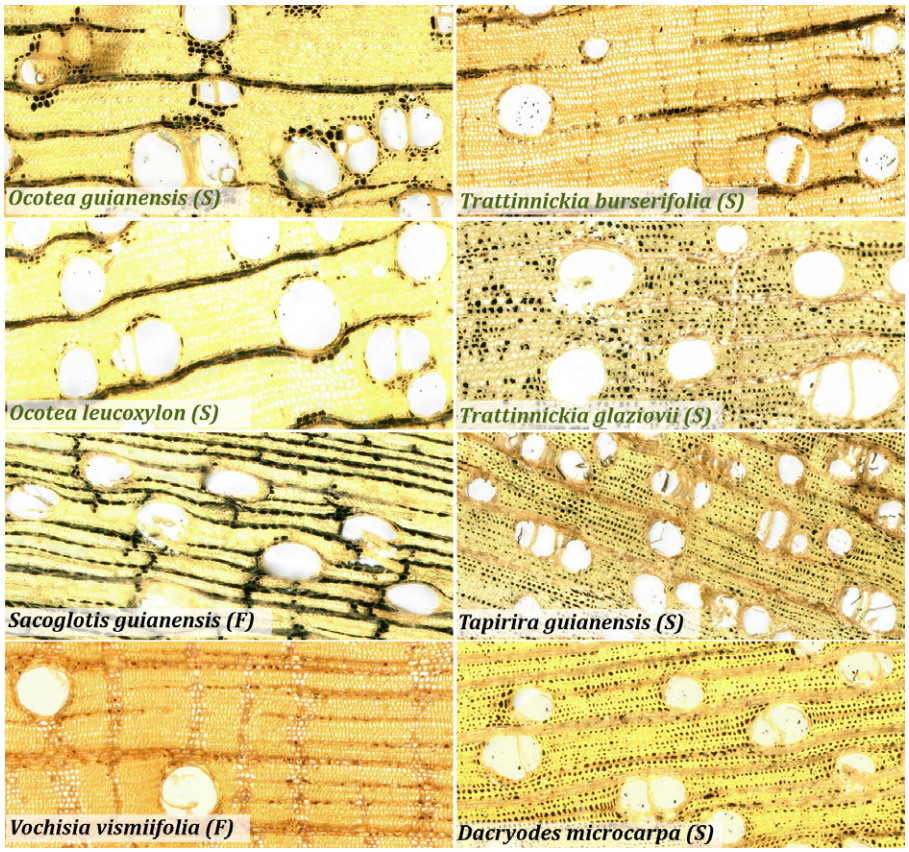

Fig. 4 Wood anatomy of the eight species successfully analyzed using our histological method. Starch grains are stained black by Lugol's iodine. The group of species on the left-hand side almost exclusively use the ray and axial parenchyma for storing starch, while the species in the right-hand side mostly use living fibers in the xylem. The upper four species (names in green) are evergreen, and the lower four (names in black) are semi-deciduous species. We also indicate fast growing species (F) and slow growing species (S) as described in Table 1.

Arnon, 1963; Yamada *et al.*, 2011; Carlquist, 2013; Plavcová *et al.*, 2016). In the individuals of the four fiber-storing species we studied here, living fibers seemed to have lived for several years as they were still functional (e.g. packed with starch) throughout the sapwood, as far as the deepest and oldest wood layers containing starch, which were from 10 to 40 years old. Our results indicate that for some tropical species, NSC storage in tree stems may be determined not only by the percentage of ray and axial parenchyma (Plavcová & Jansen, 2015), but also by the amount of living fibers (Plavcová *et al.*, 2016).

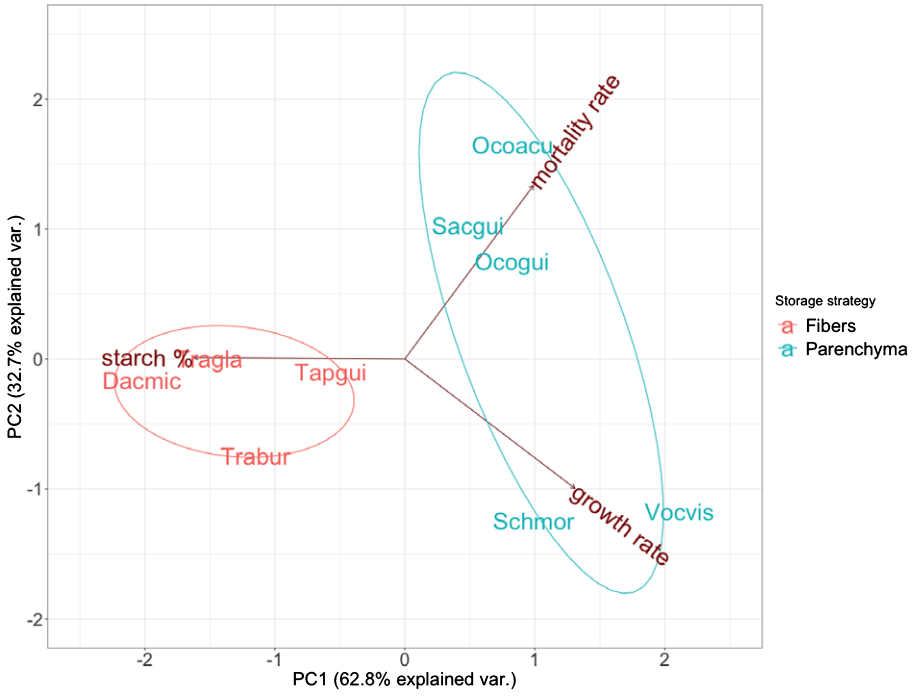

Fig. 5 Principal component analysis (PCA) between the percentage of starch in the wood, annual growth rates and mortality rates. In the plot two groups can be observed: the parenchyma storing species, *Sacoglottisguianensis* (Sacgui), *Ocotealeucoxylon* (Ocoacu), *Ocoteaguianensis* (Ocogui), *Vochysiavismiifolia* (Vocvis) and *Scheffleramorototoni* (Schmor); and the fiber storing species, *Dacryodesmicrocarpa* (Dacmic), *Trattinnickiaglaziovii* (Tragla), *Trattinnickia burserifolia* (Trabur) and *Tapirira guianensis* (Tapgui). The parenchyma storing species are grouped on the right towards high growth and mortality values. The fiber storing species are grouped on the left towards low values of growth and mortality, and high values of starch concentration.

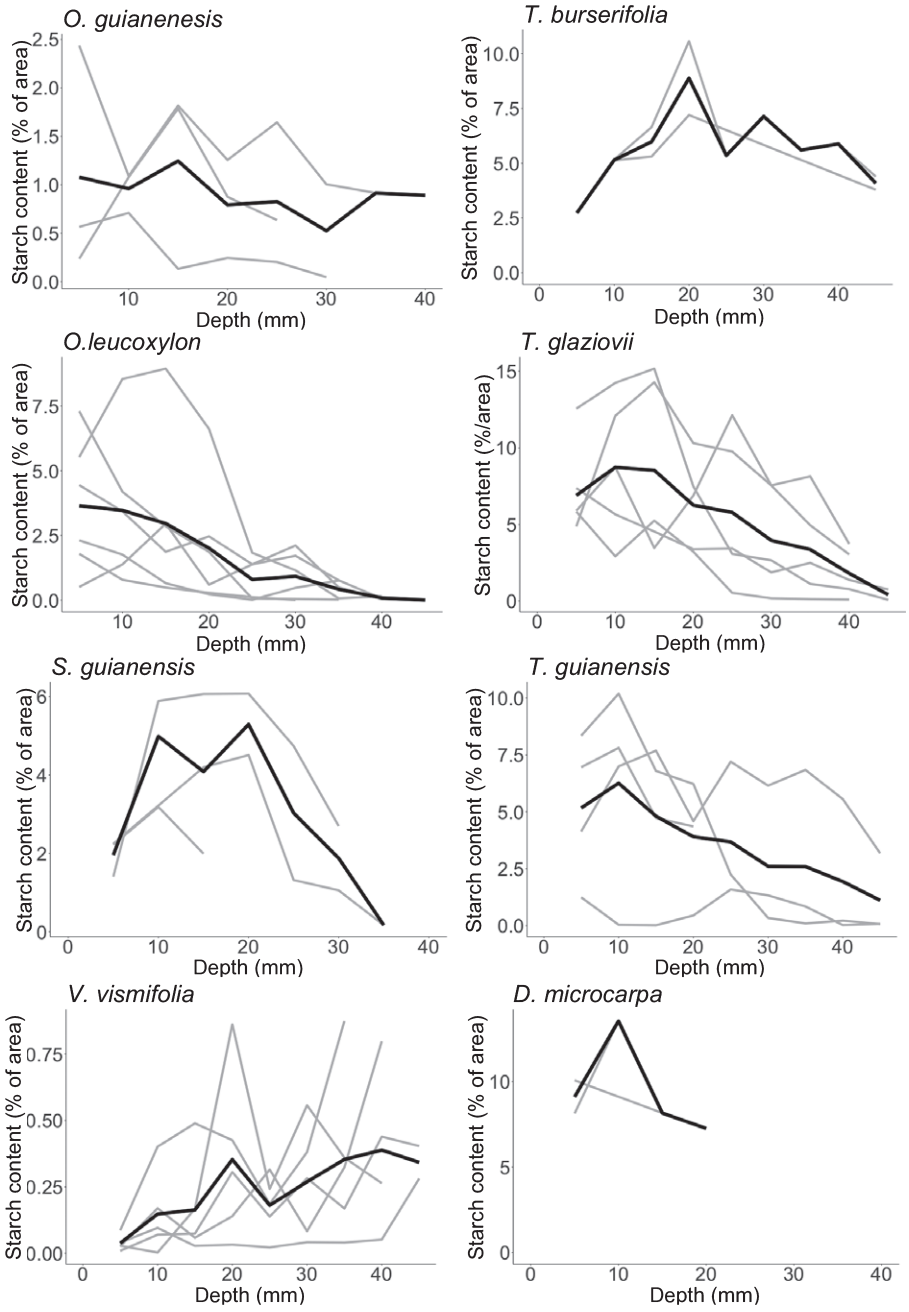

Fig. 6 Radial profile of the concentration of starch for each species (black lines) and for each individual (grey lines), measured in the first radial 4 cm of wood every 0.5 cm.

Storing starch in living fibers may be associated with slow mobilization rates, which may cause slower consumption of NSC from wood and may result in slower NSC cycling in comparison to storing starch in the parenchyma. These wood storage traits would play an important role for both the amount of starch stored and the capacity of trees to mobilize it. Slow mobilization of starch in the fiber-storing trees may be due to the physical characteristics of the living fibers (e.g. few extensive pits) and their axial disposition, which may limit the lateral movement of hydrolyzed starch (Carlquist, 2013). Fast radial transport of sugars to the phloem happens through ray parenchyma (Höll, 1975). Therefore, we speculate that hydrolyzed starch from fibers has to reach ray parenchyma before being efficiently mobilized to the phloem, which may require additional time in comparison with starch that was already stored in parenchyma cells. As a result, trees that store starch in fibers may have slower cycling of NSC, evidenced in higher quantities of old NSC stored in the wood in comparison to trees that store starch in parenchyma cells. Alternatively, the NSC may be sequestered and not readily mobilizable. For instance, mechanistic models of C allocation have shown that some tree species cycle NSC slower than others: for example, *Acer rubrum* trees, which usually have a large number of living fibers, may have slower consumption of NSC from wood and a higher quantity of old NSC stored in the wood than *Pinus taeda* trees (Carlquist, 2015; Plavcová *et al.*, 2016; Herrera-Ramírez *et al.*, 2020). Yet the variability of the anatomical

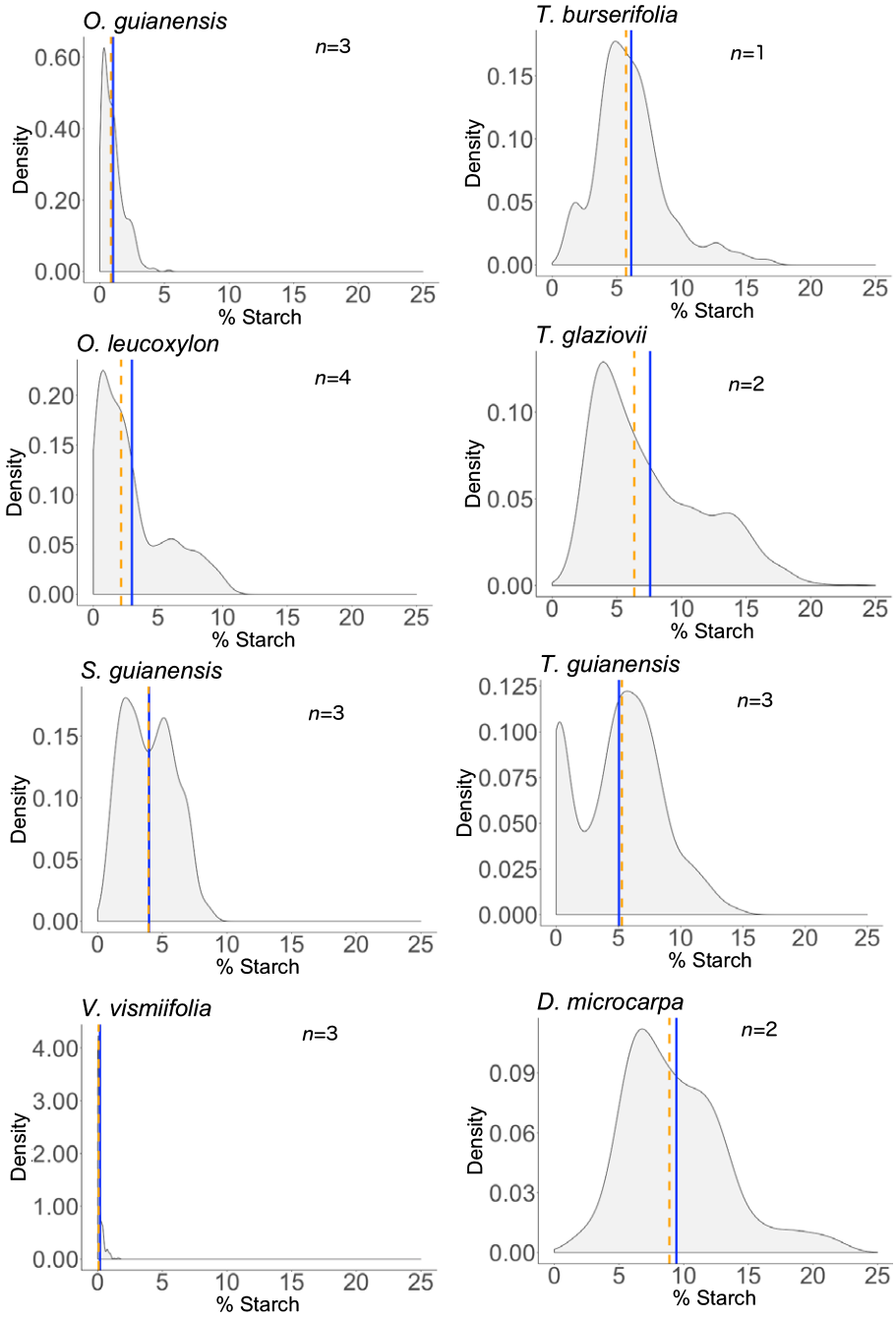

Fig. 7 The density distribution of the areal percentage of starch across the surface of the wood samples for each species, over the first 2 cm of the stem-wood radius (grey areas); the blue lines indicate the mean value of each distribution, and the orange dotted lines indicate the median of each distribution; n represents the number of individuals from each species used for the estimation of the density functions. On the left-hand side are the species that store starch in the parenchyma, and on the right-hand side are the species that mainly store starch in the fibers. The overlapping area index between the starch density distributions from parenchyma-storing species and starch-storing species is 39%, with an error $< 2.9 \times 10^{-5}$ (Supporting Information Fig. S1).

features of the living fibers and their role in the NSC cycling in trees are not well documented.

By contrast, individuals from fast-growing, short-lived and low-survival species stored starch almost exclusively in the parenchyma and had the smallest NSC pools in our study. Storing starch in the parenchyma may limit the size of the storage pool in trees, but it can increase accessibility and facilitate mobilization of reserves to promote fast growth. This may be because ray and axial parenchyma are thin-walled cells with multiple extended pits that interconnect them with other cells, including vessels (Carlquist, 2015).

Ray and axial parenchyma have additional important functions other than carbon storage, such as acting as storage reservoirs for water (Borchert & Pockman, 2005; Oliva Carrasco *et al.*, 2014), lipids (Saranpää & Höll, 1989; Hoch *et al.*, 2003) or defense compounds (Morris *et al.*, 2016; Huang *et al.*, 2020). This may explain why not all individuals from fast-growing pioneer species stored high quantities of starch, despite having a high proportion of parenchyma in their wood (e.g. *S. morototoni* and *V. vismiifolia*). For individuals from these two species, soluble sugars may play a more dominant role than starch, although in both cases the total NSC concentration was very low (Fig. 2). Individuals from these species also stored lipids, although very little compared to other species and probably not higher than the soluble sugar pool (between 1 and 2% of the wood volume as a rough estimate based on the images, Fig. 7). It may be possible that starch storage in these trees is very seasonal and spikes during other times of the year.

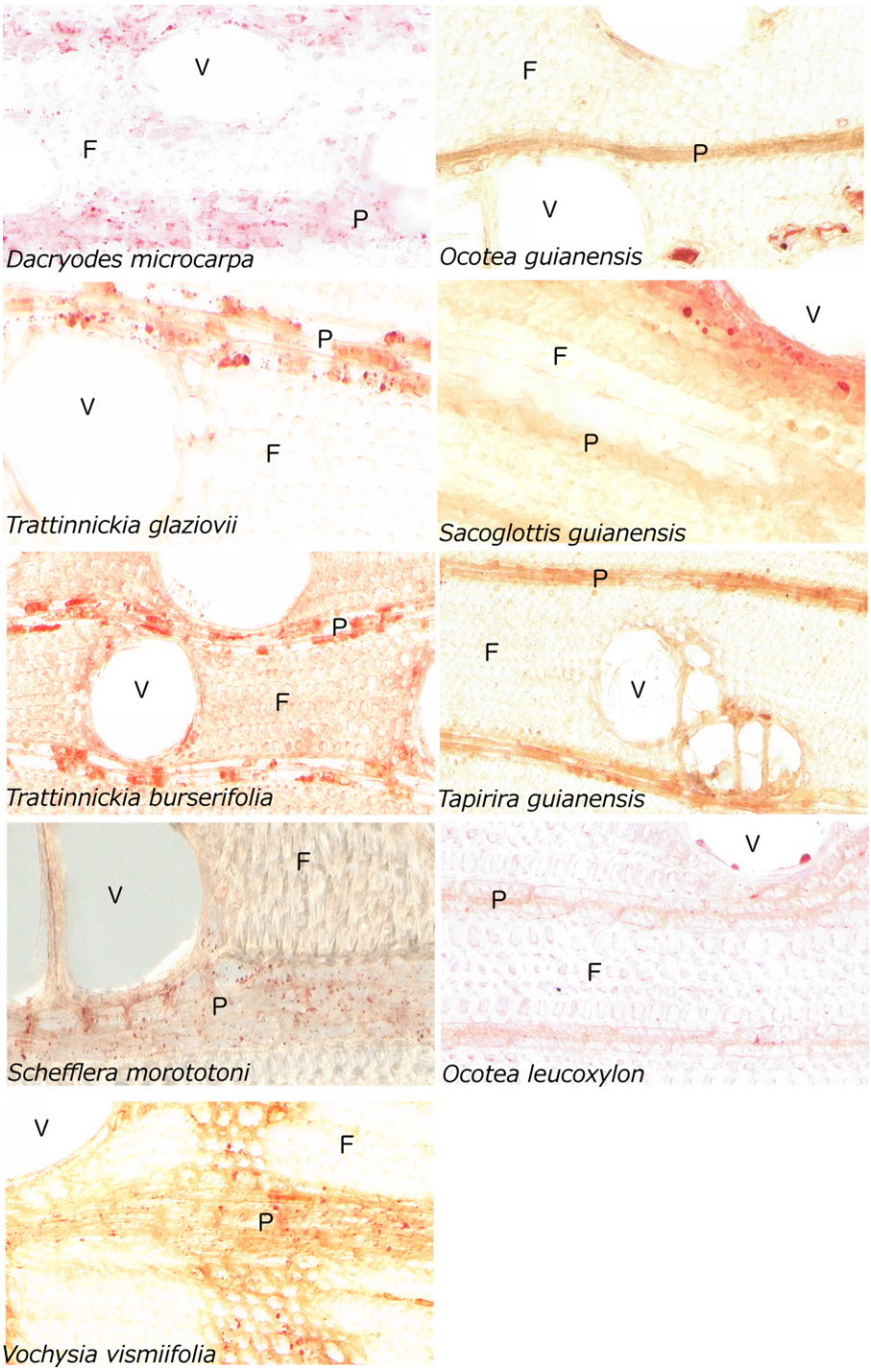

Fig. 8 Detection of neutral lipids in the stem wood of the nine species under study. Neutral lipids are visible as red droplets in the wood tissues (parenchyma cells (P), fibers (F) and vessels (V)). On the left-hand side we pooled together the species for which neutral lipids were visible all over the sampled area. They are organized from top to bottom such that the species in which neutral lipid droplets were most abundant across the sampled tissue is positioned at the top, and the species with the lowest amount of lipid droplets is positioned at the bottom. For these species, neutral lipids were exclusively localized in the ray and axial parenchyma cells. On the right-hand side we show species that exhibited very few or no neutral lipid droplets; when droplets were present, they were usually localized in the walls of vessels, as seen in *Ocotealeucoxylon* and *Sacoglottisguianensis*, or in the secretory cells, as seen in *Ocoteaguianensis*.

Nevertheless, the samples taken during the dry season suggest that *V. vismiifolia* does not store high amounts of starch during this time of the year (Fig. S1), which is probably also the case for *S. morototoni* (unfortunately, *S. morototoni* samples also showed extensive contamination with fungi). Starch storage in the stem wood may not be a priority for these fast-growing pioneer species, but it may be more pronounced in other tissue and organs such as phloem, branches and leaves where reserves are more easily accessible to maintain a fast growth rate.

Spatial distribution of starch in wood

The spatial distribution of starch in wood transversal area differed among trees of different species, and it was related to the previously identified storage strategies, annual growth and mortality rates (Figs 7, S3–S5). Trees that store starch in the living fibers showed wider distributions of starch concentration, which reflected a more dispersed pattern of starch storage in the wood, in comparison with trees that only used parenchyma for storing

starch. In our trees, starch content decreased radially along the wood core from bark to pith. This radial decrease in starch content has been documented for several species (Saranpää & Höll, 1989; Hoch *et al.*, 2003; Würth *et al.*, 2005). Nevertheless, this pattern was highly variable between trees, where some stored starch deeper than others (Fig. 6). Ultimately, this radial pattern in starch concentration determines the starch pool size, which may be more strongly related to tree survival than the average starch concentration in wood (Fig. S5). This variability in the spatial distribution of starch can be related to wood anatomical traits such as the size and abundance of parenchyma cells and living fibers (Plavcová *et al.*, 2016; Earles *et al.*, 2018; Furze *et al.*, 2020). It also may introduce strong differences between the NSC pool size and NSC mobilization between tree species, which may have large implications for tree survival and growth. These links are deserving of further research, to understand NSC dynamics in tropical trees and to confirm the patterns that we observed. Thus, more attention should be given to the quantification of the spatial distribution of starch in stem wood to better understand the role of the NSC in survival during stressful conditions.

Neutral lipids

Neutral lipid droplets contributed to tree carbon storage in five of the studied species (Fig. 8). In these trees, intricate storage patterns between lipid and starch storage were observed. Trees that store starch mostly in fibers, or those storing a very small amount of starch in parenchyma (e.g. individuals of *S. morototoni* and *V. vismiifolia*) showed lipid droplets exclusively in the parenchyma cells. This suggests that living fibers may be specialized only in starch storage. Furthermore, fiber-storing trees showed bigger and more abundant lipid droplets than individuals of *S. morototoni* and *V. vismiifolia*. This is not consistent with the separation of 'fat' tree species and 'starch' tree species (Hillinger *et al.*, 1996; Hartmann & Trumbore, 2016) as species with greater amounts of starch also showed more abundant and bigger lipid droplets. Yet starch was more abundant and more evenly distributed in the wood than lipid droplets for these species. By contrast, trees that stored starch in the parenchyma were more consistent with the 'fat' vs 'starch' tree dichotomy, and starch storage in the parenchyma cells (*O. guianensis, O. leucoxylon* and *S. guianensis*) apparently left no space for lipid droplets, suggesting that these species may rely exclusively on starch storage for supporting metabolism. Instead, trees from fast growing species that had very small starch storage and bigger parenchyma cells (*S. morototoni* and *V. vismiifolia*) showed small and dispersed lipid droplets in the parenchyma. Although our findings suggest that the presence of lipid droplets is not related to growth or functional type in the species under study here ($P = -0.11$), they seemed to be related to mortality rates ($P = 0.03$); trees that stored lipid droplets in the parenchyma were from species with lower mortality rates than trees that had no lipids. The quantification of the spatial distribution and seasonality of lipid droplets in wood may thus contribute to better predicting tree survival under constraining environmental conditions; however, the underlying mechanisms and implications for forest dynamics require further investigation.

Limitations of the histological method

We would like to stress that the histological method is not suitable for accurately quantifying starch in individuals infected with fungi or any substance that appears black upon staining in the anatomical slices. Glucans in the fungal cell wall also stain black or purple with Lugol's iodine, impairing the differentiation between fungus mycelia and starch grains (Garcia-Rubio *et al.*, 2020). Additionally, we do not know if the glucans in the fungal cell wall are also extracted by the enzymatic digestion of starch, where glucans are converted to glucose by amyloglucosidase. In this case, we would also expect an overestimation of starch content in samples from individuals infected with fungi (e.g. *S. morototoni* in Fig. 2) when standard quantification methods are applied.

Conclusions and outlook

Our results open research avenues for advancing our understanding of starch and lipid metabolism in adult trees. The histological method provides a novel and easy way to map starch and lipids in wood and understand plant storage strategies that may play an important role in survival under stressful conditions. Although our results indicate that there are links between wood storage traits, such as starch storage distribution and lipid storage, and life history traits for adult trees of nine tropical species, a more general pattern for multiple species and ecosystems still needs further investigation. We hypothesize that these relations hold for other tree species across the tropics, and the method we have presented here can help to further examine this hypothesis.

Acknowledgements

Our heartfelt thanks to the generosity of Professor Fritz Schweingruber, who supported a research stay by DH-R and actively participated in the conception of this work, design of the experiments and details of the measurements that helped answer our questions. We want to thank Leonardo Maracahipes and the IPAM team for all the support in the field and helpful advice over the selection of the species; Iris Kuhlmann, Janin Naumann and Mohammad Pouresmaeily for all the support in the lab; and Paula Sierra for producing Fig. 1. Our financial support was provided by the Max Planck Society; the Friedrich-Schiller University; the German Research Foundation (SI 1953/2-1); funding from the EU, through the German Bundesanstalt für Landwirtschaft und Ernährung FKZ: 2816ERA03W (to Susan Trumbore); and the Brazilian Council for Scientific and Technological Development – CNPq (PELD/ CNPq no. 441703/2016-0; UNIVERSAL no.430149/2018-2).

Author contributions

DH-R conceived the idea for this study. DH-R, CAS, CR, ST, JM, DS, PB and HH contributed to the design of the experiments. DH-R performed the sample analysis and quantification. DH-R wrote the manuscript. PB and DS provided the leaf phenology and growth data. DH-R, CAS, CR, ST, JM, DS, PB and

HH revised the manuscript and gave important and critical input.

ORCID

Paulo M. Brando https://orcid.org/0000-0001-8952-7025
Henrik Hartmann https://orcid.org/0000-0002-9926-5484
David Herrera-Ramírez https://orcid.org/0000-0001-6183-8032
Jan Muhr https://orcid.org/0000-0001-5264-0243
Christine Römermann https://orcid.org/0000-0003-3471-0951
Carlos A. Sierra https://orcid.org/0000-0003-0009-4169
Divino Silvério https://orcid.org/0000-0003-1642-9496
Susan Trumbore https://orcid.org/0000-0003-3885-6202

References

Adler PB, Salguero-Gomez R, Compagnoni A, Hsu JS, Ray-Mukherjee J, Mbeau-Ache C, Franco M. 2014. Functional traits explain variation in plant life history strategies. *Proceedings of the National Academy of Sciences, USA* **111**: 740–745.

von Arx G, Arzac A, Fonti P, Frank D, Zweifel R, Rigling A, Galiano L, Gessler A, Olano JM. 2017. Responses of sapwood ray parenchyma and non-structural carbohydrates of *Pinus sylvestris* to drought and long-term irrigation. *Functional Ecology* **31**: 1371–1382.

von Arx G, Crivellaro A, Prendin AL, Čufar K, Carrer M. 2016. Quantitative wood anatomy-practical guidelines. *Frontiers in Plant Science* **7**: 781.

Balch JK, Nepstad DC, Brando PM, Curran LM, Portela O, De Carvalho O, Lefebvre P. 2008. Negative fire feedback in a transitional forest of southeastern Amazonia. *Global Change Biology* **14**: 2276–2287.

Balch JK, Nepstad DC, Curran LM, Brando PM, Portela O, Guilherme P, Reuning-Scherer JD, de Carvalho O. 2011. Size, species, and fire behavior predict tree and liana mortality from experimental burns in the Brazilian Amazon. *Forest Ecology and Management* **261**: 68–77.

Begum S, Nakaba S, Oribe Y, Kubo T, Funada R. 2010. Changes in the localization and levels of starch and lipids in cambium and phloem during cambial reactivation by artificial heating of main stems of *Cryptomeria japonica* trees. *Annals of Botany* **106**: 885–895.

Boonman CCF, van Langevelde F, Oliveras I, Couédon J, Luijken N, Martini D, Veenendaal EM. 2020. On the importance of root traits in seedlings of tropical tree species. *New Phytologist* **227**: 156–167.

Borchert R, Pockman WT. 2005. Water storage capacitance and xylem tension in isolated branches of temperate and tropical trees. *Tree Physiology* **25**: 457–466.

Borghetti M, Gentilesca T, Colangelo M, Ripullone F, Rita A. 2020. Xylem functional traits as indicators of health in Mediterranean forests. *Current Forestry Reports* **6**: 220–236.

Brando PM, Silvério D, Maracahipes-Santos L, Oliveira-Santos C, Levick SR, Coe MT, Migliavacca M, Balch JK, Macedo MN, Nepstad DC *et al.* 2019. Prolonged tropical forest degradation due to compounding disturbances: implications for CO_2 and H_2O fluxes. *Global Change Biology* **25**: 2855–2868.

Carlquist S. 2013. Fibre dimorphism: cell type diversification as an evolutionary strategy in angiosperm woods. *Botanical Journal of the Linnean Society* **174**: 44–67.

Carlquist S. 2015. Living cells in wood. 1. Absence, scarcity and histology of axial parenchyma as keys to function. *Botanical Journal of the Linnean Society* **177**: 291–321.

Chapin FS, Schulze E, Mooney HA. 1990. The ecology and economics of storage in plants. *Annual Review of Ecology and Systematics* **21**: 423–447.

Chesney P, Vasquez N. 2007. Dynamics of non-structural carbohydrate reserves in pruned *Erythrina poeppigiana* and *Gliricidia sepium* trees. *Agroforestry Systems* **69**: 89–105.

Czemmel S, Galarneau ER, Travadon R, McElrone AJ, Cramer GR, Baumgartner K. 2015. Genes expressed in grapevine leaves reveal latent wood infection by the fungal pathogen *Neofusicoccum parvum*. *PLoS ONE* **10**: 1–21.

Datta SK, Kumar A. 1987. Histochemical studies of the transition from sapwood to heartwood in *Tectona Grandis*. *IAWA Journal* **8**: 363–368.

Dickman LT, McDowell NG, Grossiord C, Collins AD, Wolfe BT, Detto M, Wright SJ, Medina-Vega JA, Goodsman D, Rogers A *et al.* 2019. Homoeostatic maintenance of nonstructural carbohydrates during the 2015–2016 El Niño drought across a tropical forest precipitation gradient. *Plant, Cell & Environment* **42**: 1705–1714.

Earles JM, Knipfer T, Tixier A, Orozco J, Reyes C, Zwieniecki MA, Brodersen CR, McElrone AJ. 2018. *In vivo* quantification of plant starch reserves at micrometer resolution using X-ray microCT imaging and machine learning. *New Phytologist* **218**: 1260–1269.

Fahn A, Arnon N. 1963. The living wood fibres of *Tamarix aphylla* and the changes occurring in them in transition from sapwood to heartwood. *New Phytologist* **62**: 99–104.

Fischer C, Höll W. 1991. Food reserves of Scots pine (*Pinus sylvestris* L.). *Trees* **5**: 187–195.

Fischer S, Hanf S, Frosch T, Gleixner G, Popp J, Trumbore S, Hartmann H. 2015. *Pinus sylvestris* switches respiration substrates under shading but not during drought. *New Phytologist* **207**: 542–550.

Furze ME, Huggett BA, Aubrecht DM, Stolz CD, Carbone MS, Richardson AD. 2019. Whole-tree nonstructural carbohydrate storage and seasonal dynamics in five temperate species. *New Phytologist* **221**: 1466–1477.

Furze ME, Huggett BA, Chamberlain CJ, Wieringa MM, Aubrecht DM, Carbone MS, Walker JC, Xu X, Czimczik CI, Richardson AD. 2020. Seasonal fluctuation of nonstructural carbohydrates reveals the metabolic availability of stemwood reserves in temperate trees with contrasting wood anatomy. *Tree Physiology* **40**: 1355–1365.

Furze ME, Trumbore S, Hartmann H. 2018. Detours on the phloem sugar highway: stem carbon storage and remobilization. *Current Opinion in Plant Biology* **43**: 89–95.

Garcia-Rubio R, de Oliveira HC, Rivera J, Trevijano-Contador N. 2020. The fungal cell wall: *Candida*, *Cryptococcus*, and *Aspergillus* species. *Frontiers in Microbiology* **10**: 2993.

Gérard B, Bréda N. 2014. Radial distribution of carbohydrate reserves in the trunk of declining European beech trees (*Fagus sylvatica* L.). *Annals of Forest Science* **71**: 675–682.

Gilbert B, Wright SJ, Muller-Landau HC, Kitajima K, Hernandéz A. 2006. Life history trade-offs in tropical trees and lianas. *Ecology* **87**: 1281–1288.

Hartmann H, Trumbore S. 2016. Understanding the roles of nonstructural carbohydrates in forest trees – from what we can measure to what we want to know. *New Phytologist* **211**: 386–403.

Herrera-Ramírez D, Muhr J, Hartmann H, Römermann C, Trumbore S, Sierra CA. 2020. Probability distributions of nonstructural carbon ages and transit times provide insights into carbon allocation dynamics of mature trees. *New Phytologist* **226**: 1299–1311.

Hillinger C, Höll W, Ziegler H. 1996. Lipids and lipolytic enzymes in the trunkwood of *Robinia pseudoacacia* L. during heartwood formation: I. Radial distribution of lipid classes. *Trees* **10**: 366–375.

Hoch G, Richter A, Körner Ch. 2003. Non-structural carbon compounds in temperate forest trees. *Plant, Cell & Environment* **26**: 1067–1081.

Höll W. 1975. Radial transport in rays. In: Zimmermann MH, Milburn JA, eds. *Transport in plants I*. Berlin/Heidelberg, Germany: Springer, 432–450.

Höll W, Poschenrieder G. 1975. Radial distribution and partial characterization of lipids in the trunk of three hardwoods. *Holzforschung* **29**: 118–123.

Huang J, Kautz M, Trowbridge AM, Hammerbacher A, Raffa KF, Adams HD, Goodsman DW, Xu C, Meddens AJH, Kandasamy D *et al.* 2020. Tree defence and bark beetles in a drying world: carbon partitioning, functioning and modelling. *New Phytologist* **225**: 26–36.

Johnson DM, McCulloh KA, Woodruff DR, Meinzer FC. 2012. Hydraulic safety margins and embolism reversal in stems and leaves: why are conifers and angiosperms so different? *Plant Science* **195**: 48–53.

Landhäusser SM, Chow PS, Dickman LT, Furze ME, Kuhlman I, Schmid S, Wiesenbauer J, Wild B, Gleixner G, Hartmann H *et al.* 2018. Standardized

protocols and procedures can precisely and accurately quantify non-structural carbohydrates. *Tree Physiology* **38**: 1764–1778.

Lintunen A, Paljakka T, Jyske T, Peltoniemi M, Sterck F, von Arx G, Cochard H, Copini P, Caldeira MC, Delzon S *et al.* 2016. Osmolality and non-structural carbohydrate composition in the secondary phloem of trees across a latitudinal gradient in Europe. *Frontiers in Plant Science* **7**: 726.

McDowell N, Pockman WT, Allen CD, Breshears DD, Cobb N, Kolb T, Plaut J, Sperry J, West A, Williams DG *et al.* 2008. Mechanisms of plant survival and mortality during drought: why do some plants survive while others succumb to drought? *New Phytologist* **178**: 719–739.

Mehlem A, Hagberg CE, Muhl L, Eriksson U, Falkevall A. 2013. Imaging of neutral lipids by oil red O for analyzing the metabolic status in health and disease. *Nature Protocols* **8**: 1149–1154.

Morris H, Brodersen C, Schwarze FWMR, Jansen S. 2016. The parenchyma of secondary xylem and its critical role in tree defense against fungal decay in relation to the CODIT model. *Frontiers in Plant Science* **7**: 1665.

Nobuchi T, Janmahasatien S, Sakai M. 1996. Seasonal changes of wood formation and some characteristics of heartwood formation in teak (*Tectona grandis* L.) plantation. *Kasetsart Journal – Natural Science* **30**: 254–262.

O'Brien MJ, Burslem DFRP, Caduff A, Tay J, Hector A. 2014. Contrasting nonstructural carbohydrate dynamics of tropical tree seedlings under water deficit and variability. *New Phytologist* **205**: 1083–1094.

O'Brien MJ, Valtat A, Abiven S, Studer MS, Ong R, Schmid B. 2020. The role of soluble sugars during drought in tropical tree seedlings with contrasting tolerances. *Journal of Plant Ecology* **13**: 389–397.

Oliva Carrasco L, Bucci SJ, Di Francescantonio D, Lezcano OA, Campanello PI, Scholz FG, Rodríguez S, Madanes N, Cristiano PM, Hao G-Y *et al.* 2014. Water storage dynamics in the main stem of subtropical tree species differing in wood density, growth rate and life history traits. *Tree Physiology* **35**: 354–365.

Osazuwa-Peters OL, Wright SJ, Zanne AE. 2017. Linking wood traits to vital rates in tropical rainforest trees: Insights from comparing sapling and adult wood. *American Journal of Botany* **104**: 1464–1473.

Philipson CD, Dent DH, O'Brien MJ, Chamagne J, Dzulkifli D, Nilus R, Philips S, Reynolds G, Saner P, Hector A. 2014. A trait-based trade-off between growth and mortality: evidence from 15 tropical tree species using size-specific relative growth rates. *Ecology and Evolution* **4**: 3675–3688.

Plavcová L, Hoch G, Morris H, Ghiasi S, Jansen S. 2016. The amount of parenchyma and living fibers affects storage of nonstructural carbohydrates in young stems and roots of temperate trees. *American Journal of Botany* **103**: 603–612.

Plavcová L, Jansen S. 2015. The role of xylem parenchyma in the storage and utilization of nonstructural carbohydrates. In: Hacke U, ed. *Functional and ecological xylem anatomy*. Cham, Switzerland: Springer International, 209–234.

Poorter L, Kitajima K. 2007. Carbohydrate storage and light requirements of tropical moist and dry forest tree species. *Ecology* **88**: 1000–1011.

Poorter L, Wright SJ, Paz H, Ackerly DD, Condit R, Ibarra-Manríquez G, Harms KE, Licona JC, Martínez-Ramos M, Mazer SJ *et al.* 2008. Are functional traits good predictors of demographic rates? Evidence from five neotropical forests. *Ecology* **89**: 1908–1920.

R Core Team. 2017. *R: A language and environment for statistical computing*. Vienna, Austria: R Foundation for Statistical Computing.

Rocha W, Metcalfe DB, Doughty CE, Brando P, Silvério D, Halladay K, Nepstad DC, Balch JK, Malhi Y. 2014. Ecosystem productivity and carbon cycling in intact and annually burnt forest at the dry southern limit of the Amazon rainforest (Mato Grosso, Brazil). *Plant Ecology & Diversity* **7**: 25–40.

Rowland L, da Costa ACL, Galbraith DR, Oliveira RS, Binks OJ, Oliveira AAR, Pullen AM, Doughty CE, Metcalfe DB, Vasconcelos SS *et al.* 2015. Death from drought in tropical forests is triggered by hydraulics not carbon starvation. *Nature* **528**: 119–122.

Sala A, Woodruff DR, Meinzer FC. 2012. Carbon dynamics in trees: feast or famine? *Tree Physiology* **32**: 764–775.

Salleo S, Trifilo P, Esposito S, Nardini A, Lo Gullo MA. 2009. Starch-to-sugar conversion in wood parenchyma of field-growing *Laurus nobilis* plants: a component of the signal pathway for embolism repair? *Functional Plant Biology* **36**: 815–825.

Saranpää P, Höll W. 1989. Soluble carbohydrates of *Pinus sylvestris* L. sapwood and heartwood. *Trees* **3**: 138–143.

Savi T, Casolo V, Luglio J, Bertuzzi S, Trifilo' P, Lo Gullo MA, Nardini A. 2016. Species-specific reversal of stem xylem embolism after a prolonged drought correlates to endpoint concentration of soluble sugars. *Plant Physiology and Biochemistry* **106**: 198–207.

Schneider CA, Rasband WS, Eliceiri KW. 2012. NIH Image to ImageJ: 25 years of image analysis. *Nature Methods* **9**: 671–675.

Schneider H, Manz B, Westhoff M, Mimietz S, Szimtenings M, Neuberger T, Faber C, Krohne G, Haase A, Volke F *et al.* 2003. The impact of lipid distribution, composition and mobility on xylem water refilling of the resurrection plant *Myrothamnus flabellifolia*. *New Phytologist* **159**: 487–505.

Smirnova J, Fernie AR, Steup M. 2015. Starch degradation. In: Nakamura Y, ed. *Starch: metabolism and structure*. Tokyo, Japan: Springer, 239–290.

Spicer R. 2014. Symplasmic networks in secondary vascular tissues: parenchyma distribution and activity supporting long-distance transport. *Journal of Experimental Botany* **65**: 1829–1848.

Sulpice R, Pyl E-T, Ishihara H, Trenkamp S, Steinfath M, Witucka-Wall H, Gibon Y, Usadel B, Poree F, Piques MC *et al.* 2009. Starch as a major integrator in the regulation of plant growth. *Proceedings of the National Academy of Sciences, USA* **106**: 10348.

Tixier A, Orozco J, Roxas AA, Earles JM, Zwieniecki MA. 2018. Diurnal variation in nonstructural carbohydrate storage in trees: remobilization and vertical mixing. *Plant Physiology* **178**: 1602.

Welte MA, Gould AP. 2017. Lipid droplet functions beyond energy storage. *Recent Advances in Lipid Droplet Biology* **1862**: 1260–1272.

Wiley E, King CM, Landhäusser SM. 2019. Identifying the relevant carbohydrate storage pools available for remobilization in aspen roots. *Tree Physiology* **39**: 1109–1120.

Wright SJ, Kitajima K, Kraft NJB, Reich PB, Wright IJ, Bunker DE, Condit R, Dalling JW, Davies SJ, Díaz S *et al.* 2010. Functional traits and the growth–mortality trade-off in tropical trees. *Ecology* **91**: 3664–3674.

Würth MKR, Peláez-Riedl S, Wright SJ, Körner C. 2005. Non-structural carbohydrate pools in a tropical forest. *Oecologia* **143**: 11–24.

Yamada Y, Awano T, Fujita M, Takabe K. 2011. Living wood fibers act as large-capacity "single-use" starch storage in black locust (*Robinia pseudoacacia*). *Trees* **25**: 607–616.

Supporting Information

Additional Supporting Information may be found online in the Supporting Information section at the end of the article.

Fig. S1 Wood anatomy of the samples taken in July 2018 from the eight species successfully analyzed by the histological method.

Fig. S2 Box plot for the comparison of the species growth rates, and the species mortality rates between the two storage strategy groups, and between the two lipid storage groups.

Fig. S3 Comparison between the starch density distributions in the stem wood of the fiber-storing trees and the parenchyma-storing trees.

Fig. S4 Relationship between the median of the annual growth rate of each sampled species and the median of the percentage of starch in the first 2 cm of the wood core.

Fig. S5 Association between mortality rates and the cumulative mean percentage of starch along the wood core from bark to 4 cm, and mortality and the mean percentage of starch.

Methods S1 Protocol for sample collection and specific staining of starch and neutral lipids on stemwood.

Methods S2 ImageJ macro for measuring percentage of starch coverage in histological images of the cross-sectional view of wood.

Please note: Wiley Blackwell are not responsible for the content or functionality of any Supporting Information supplied by the authors. Any queries (other than missing material) should be directed to the *New Phytologist* Central Office.